Electronic supplementary information (ESI) for

A room-temperature moisture-stabilized ferroelectric energetic material for piezoelectric generation

Jun Wang, Xiao-Xian Chen, Le Ye, Ya-Ping Gong, Yu Shang, Wei-Xiong Zhang*

MOE Key Laboratory of Bioinorganic and Synthetic Chemistry, School of Chemistry, Sun Yat-Sen University, Guangzhou 510275, China.

** Corresponding author.*

E-mail address: zhangwx6@mail.sysu.edu.cn (Wei-Xiong Zhang).

Syntheses details

(Hmdabco)(NH_4)(ClO_4)$_3$ (DAP-M4) was synthesized according to the method in literature [49]. Ammonium perchlorate (2 mmol) and 70% perchloric acid solution (0.7 mL) were added to H_2O (5 mL); then an aqueous solution (2 mL) of 1-methyl-1,4-diazabicyclo[2.2.2]octane-1,4-diium Iodide (2 mmol) was added into the above solution slowly. The white solid was obtained by filtration and washed three times with ethanol (70% yield based on NH_4ClO_4). The pure purity was confirmed by PXRD pattern (Figure S1).

(Ac)ClO_4 (Acetamidinium Perchlorate) was synthesized according to the method in literature [50]. The colourless crystals were obtained by slowly evaporating the aqueous solution containing equal molar of acetamidine hydrochloride and acetamidine acetate at room temperature. The phase purity was confirmed by PXRD pattern (Figure S6a).

(Im)ClO_4 (Imidazolium Perchlorate) was synthesized according to the method in literature [45]. The poly-crystalline products were obtained by evaporation of an aqueous solution containing equal molar amounts of imidazolium chloride and perchloric acid at room temperature. The phase purity was confirmed by PXRD pattern (Figure S6b).

(Hdabco)ClO_4 (1,4-diazabicyclo[2.2.2]octan-1-ium perchlorate) was synthesized according to the method in literature [3]. The poly-crystalline products were obtained by slowly evaporating the ethanol solution of dabco and $HClO_4$ in a 1:1 molar ratio at room temperature. The phase purity was confirmed by PXRD pattern (Figure S6c).

Table S1. Crystallographic data and structural refinements parameters for DAP-M4.

Complex	DAP-M4		
Formula	$C_7H_{20}Cl_3N_3O_{12}$		
Formula weight	444.61		
Temperature (K)	293.00(1)	358.5(1)	393(1)
Phase	RTP	ITP	HTP
Crystal system	monoclinic	trigonal	cubic
Space group	$P2_1$	$R\bar{3}m$	$Pm\bar{3}m$
a/Å	10.20664(1)	10.6675(8)	7.5679(4)
b/Å	11.00567(1)	10.6675(8)	7.5679(4)
c/Å	14.84750(2)	13.0585(1)	7.5679(4)
β/°	90.1263(1)	90	90
V/Å^3	1667.83(3)	1286.9(2)	433.44(7)
Z	4	3	1
D_c /(g/cm^3)	1.771	1.721	1.703
R_1[a] (> 2σ(*I*))	0.0381	0.0642	0.0602
wR_2[b](all data)	0.1032	0.2126	0.1808
GOF	1.054	1.066	1.097
Flack parameter	/ [c]	/	/
CCDC number	2234259	2234258	2234257

[a] $R_1 = \sum||F_o| - |F_c||/\sum|F_o|$, [b] $wR_2 = \{\sum w[(F_o)^2 - (F_c)^2]^2/\sum w[(F_o)^2]^2\}^{1/2}$,

[c] Twinning involves inversion (TWIN −1 0 0 0 −1 0 0 0 1 −4, BASF 0.00989 0.31381 0.02369), so Flack parameter cannot be determined.

Table S2. The DFT calculated elastic properties of DAP-M4

Mechanical Properties		Anisotropy
Young's Modulus *E* (GPa)	Min 17.082	1.386
	Max 23.684	
Shear Modulus *G* (GPa)	Min 6.574	1.461
	Max 9.603	
Poisson's Ratio *v*	Min 0.152	2.785
	Max 0.423	

Table S3. Clamped-ion ē (C/m^2) and relaxed-ion ê (C/m^2) for DAP-M4

Index	ē (C/m^2)	ê (C/m^2)
14	-0.0138	0.00741
16	0	0
21	-0.01049	0.00634
22	0.01765	-0.00052
23	0.01044	-0.00668
25	0	0
34	0.04366	0.00375
36	-0.00005	0

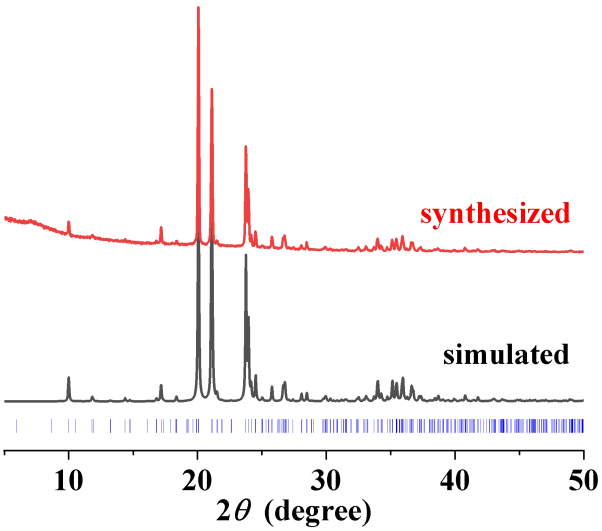

Figure S1. The experimental PXRD pattern (red) on the as-synthesized powder sample and the simulated PXRD pattern (black) based on the single-crystal structure of DAP-M4 at room temperature.

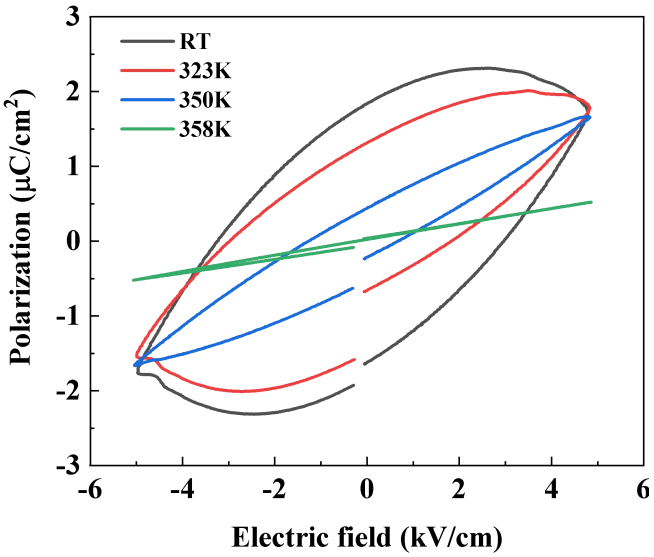

Figure S2. variable-temperature *P-E* hysteresis loops of DAP-M4.

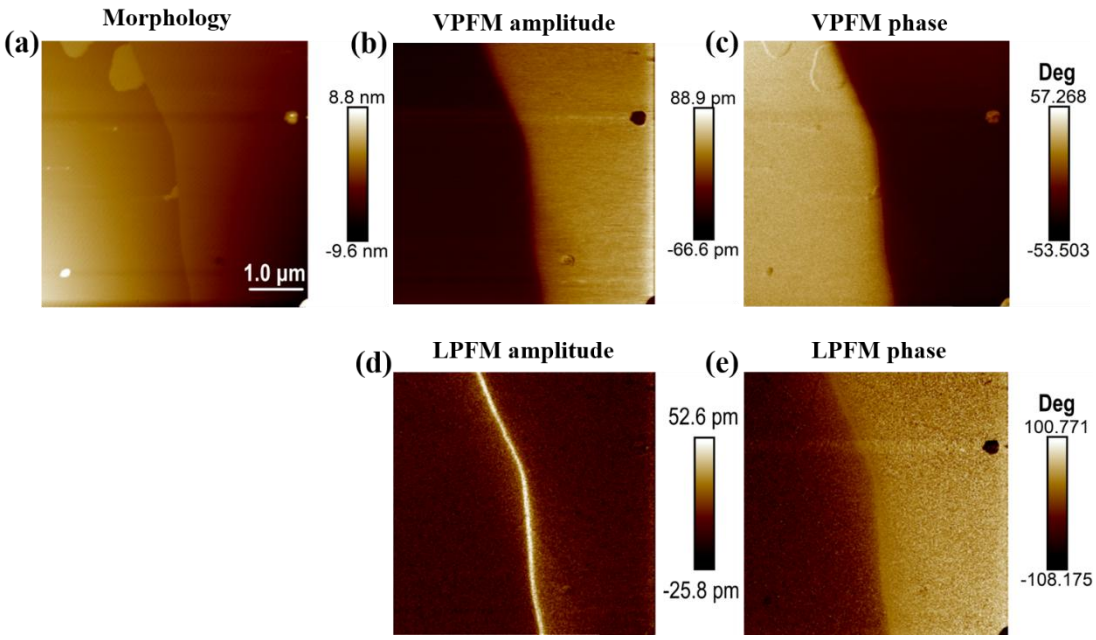

Figure S3. Morphology image (a), vertical (b, c) and Lateral (d, e) PFM images of the crystal surface for DAP-M4.

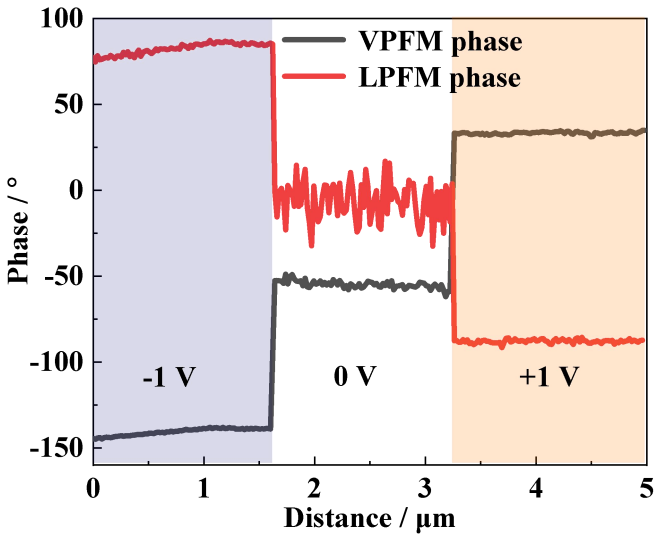

Figure S4. VPFM and LPFM Phase change with voltage variation.

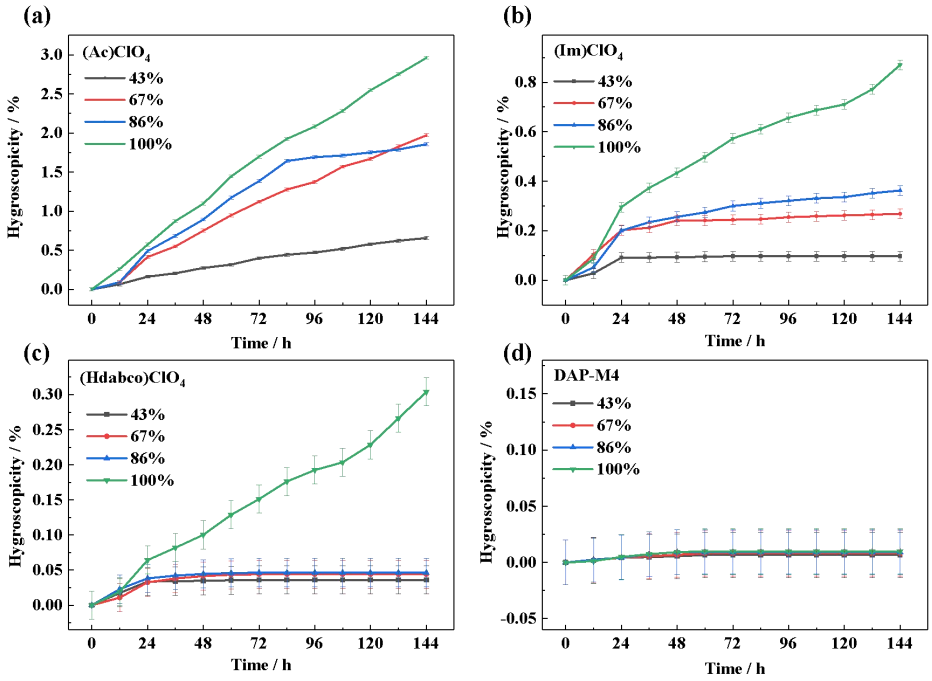

Figure S5. Hygroscopic curves of $(Ac)ClO_4$ (a), $(Im)ClO_4$ (b), $(Hdabco)ClO_4$ (c) and DAP-M4 (d) under different relative humidity at ambient temperature.

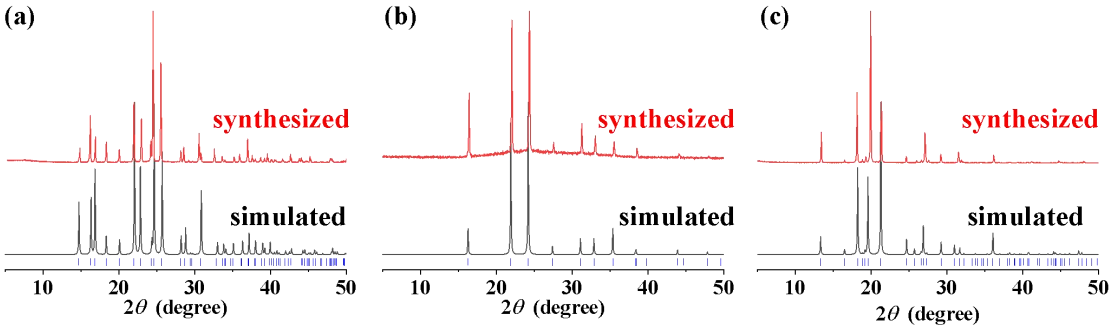

Figure S6. Experimental PXRD patterns (red) on as-synthesized powder samples and simulated PXRD patterns (black) based on single-crystal structures of $(Ac)ClO_4$ (a), $(Im)ClO_4$ (b), $(Hdabco)ClO_4$ (c).

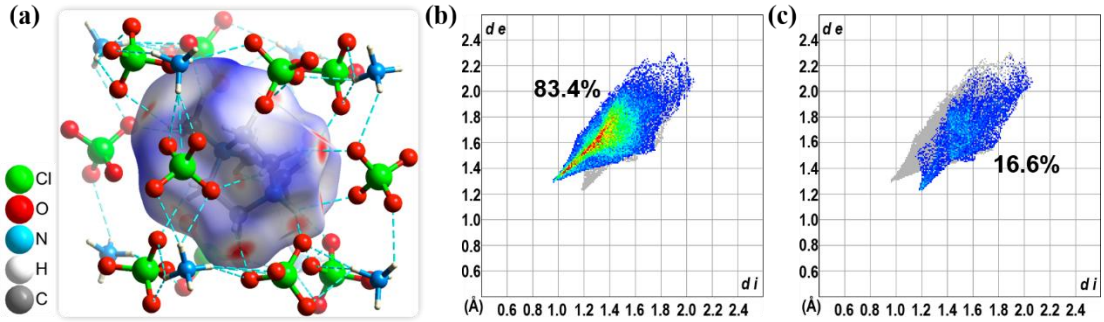

Figure S7. Hirshfeld surface for the organic cations in DAP-M4 (a), fingerprint plot for H···O contacts (b), fingerprint plot for H···H contacts (c), with d_i and d_e ranging from 0.6 to 2.4 Å.

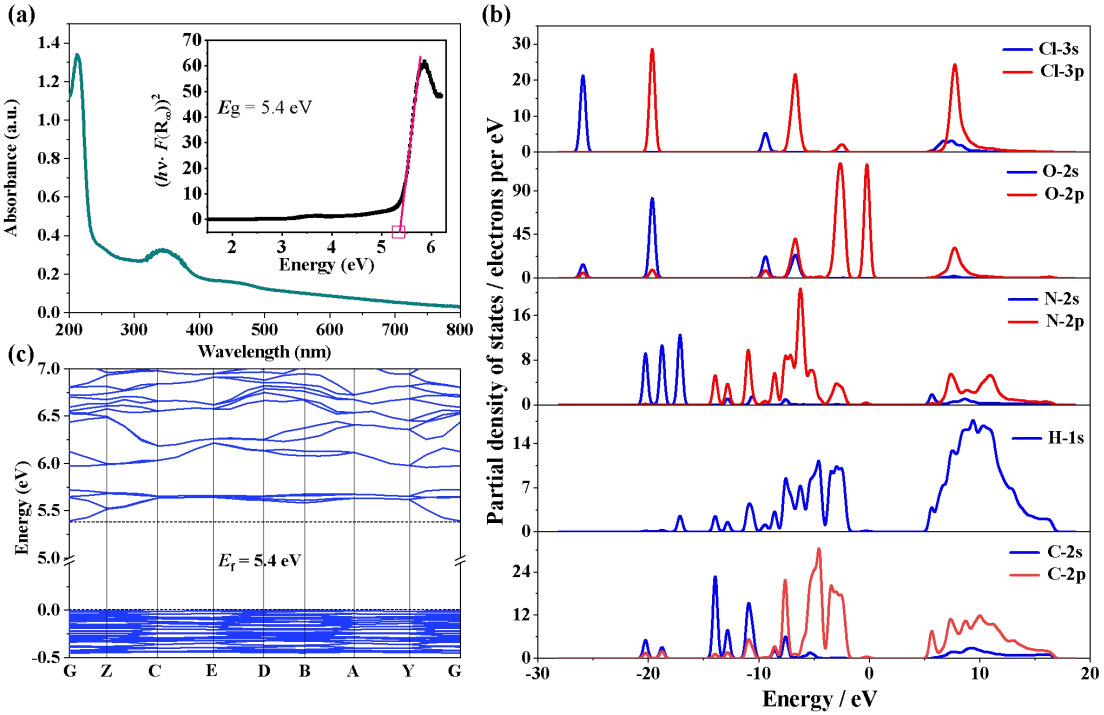

Figure S8. UV-vis absorption spectra (a) and band gap (inset), calculated PDOS (b) and band structure (c) for DAP-M4.

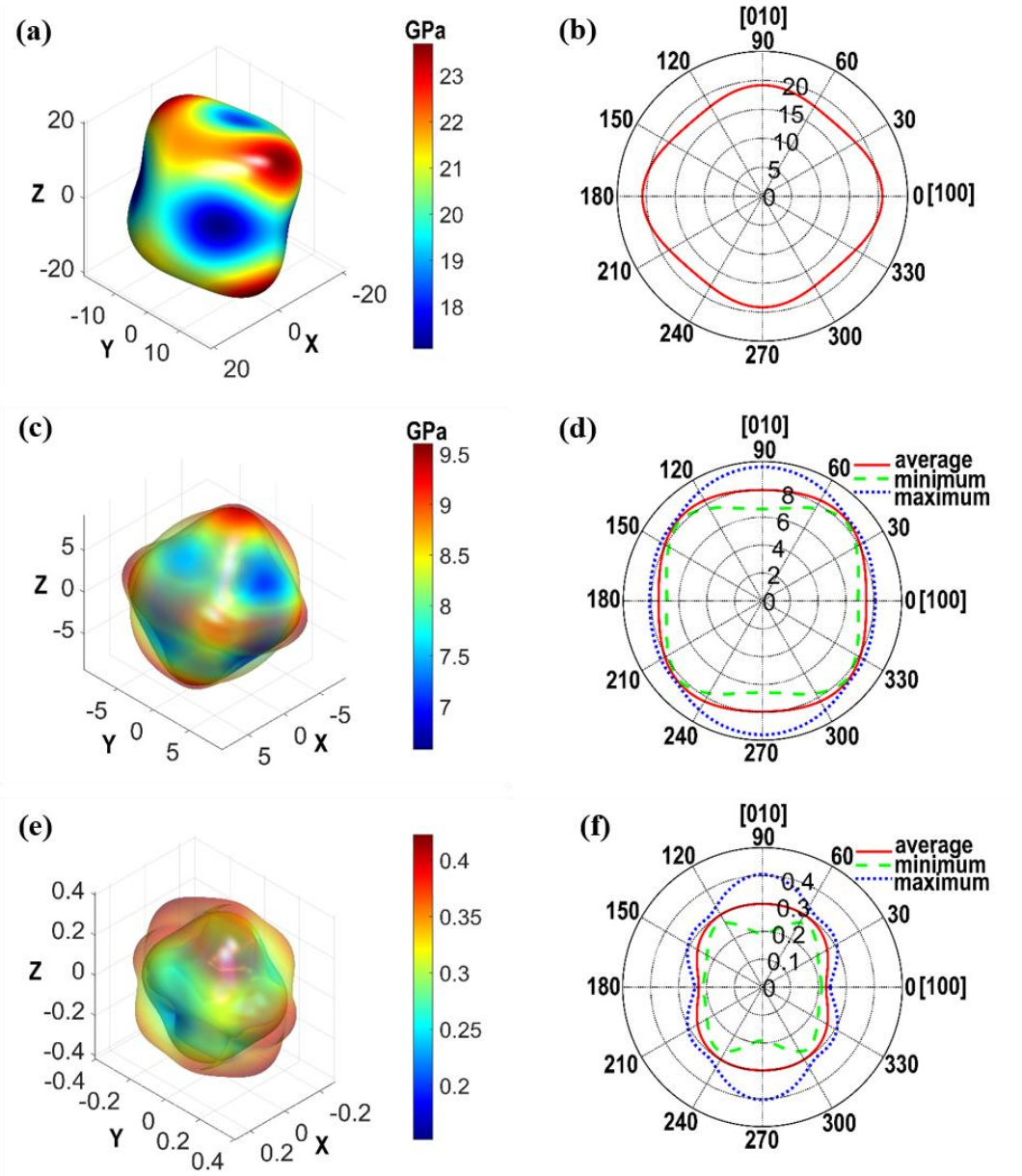

Figure S9. 3D rendering and 2D projection representations of Young's modulus (*E*) (a) and (b), shear modulus (*G*) (c) and (d), and Poisson's ratio (*v*) (e) and (f) of DAP-M4. The transparent outer layer in (c) and (e), the blue outer line in (d) and (f), represent the maximum values; the semi-transparent middle layer in (c) and (e), the red middle line in (d) and (f), represent the average values; and the non-transparent inner layer in (c) and (e), the green inner line in (d) and (f), represent the minimum values.

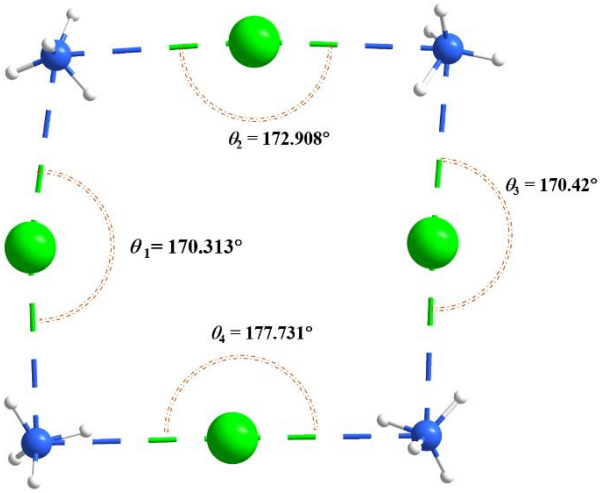

Figure S10. the bond angles of <-1 -1 0> direction for DAP-M4, the $(Hmdabco)^{2+}$ was omitted for clarity.

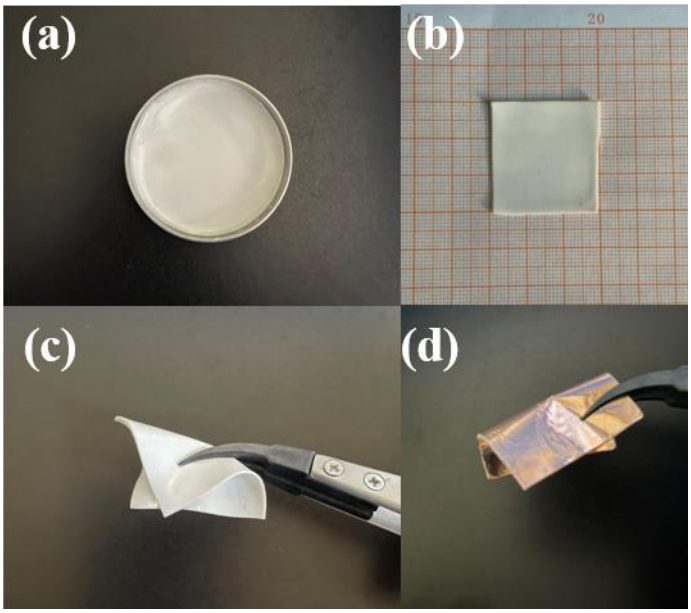

Figure S11. (a) Photograph of formed film in mould of the DAP-M4/TPU. (b) photograph of the DAP-M4/TPU film with dimension of 3 × 3 cm^2. (c) photograph of the flexible DAP-M4/TPU film. (d) photograph of the composite piezogenerator based on DAP-M4/TPU.

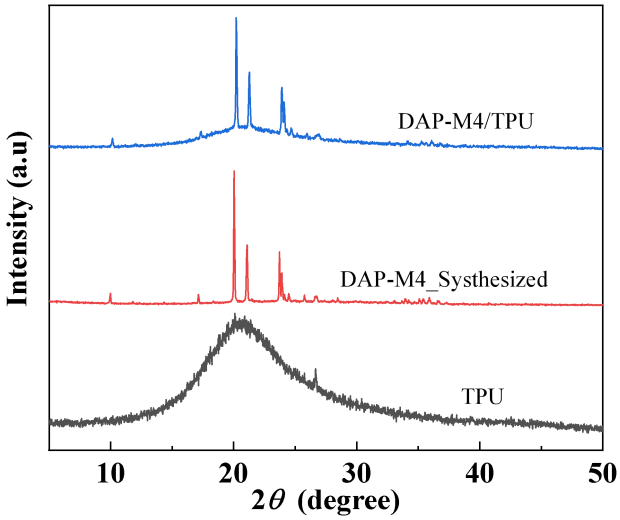

Figure S12. XRD patterns of DAP-M4/TPU films.

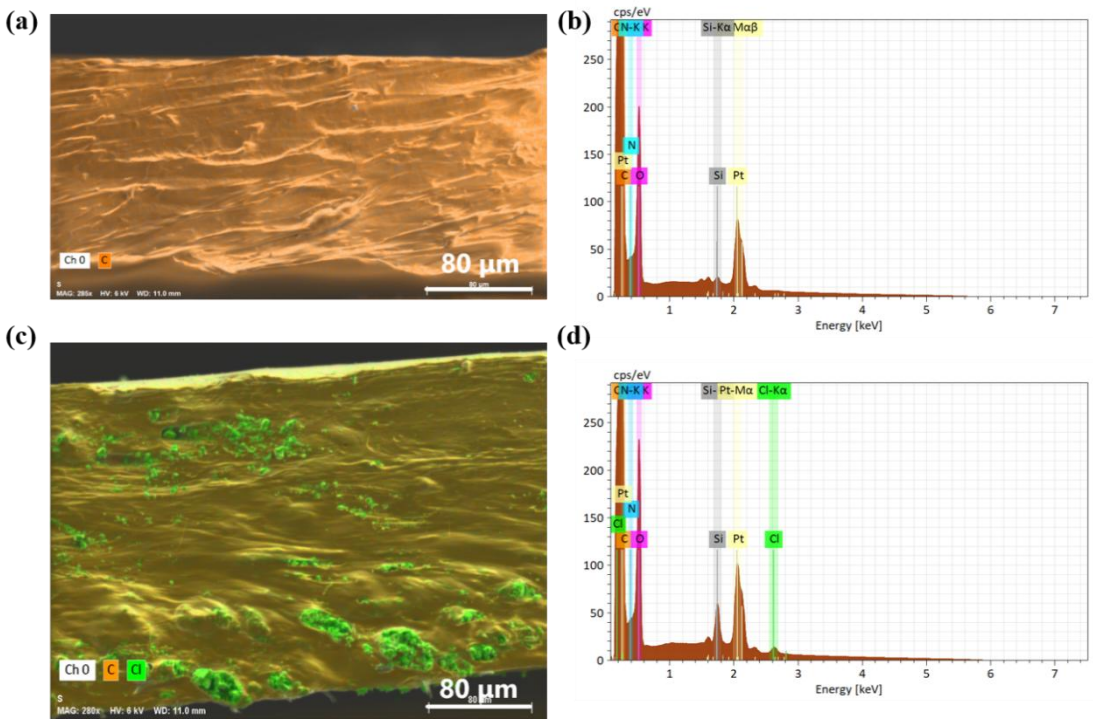

Figure S13. Cross-sectional mapping images of (a) TPU and (c) DAP-M4/TPU films, EDS spectra of (b) TPU and (d) DAP-M4/TPU films.

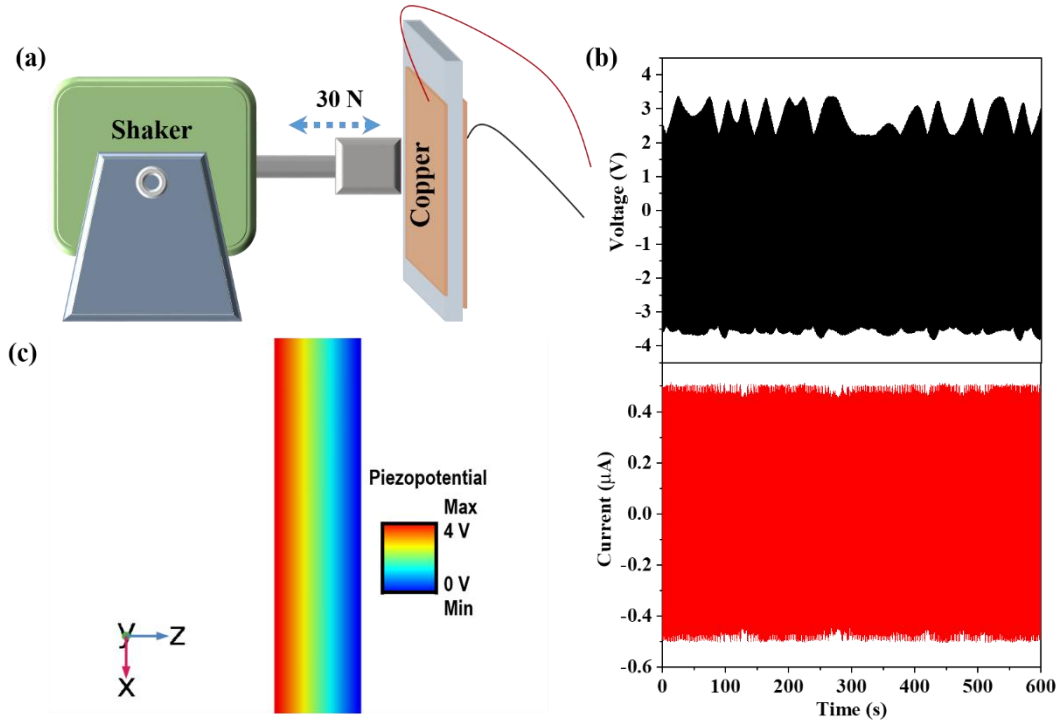

Figure S14. (a) Schematic of piezoelectric generation test. (b) open-circuit voltage (V_{oc}) and short-circuit current (I_{sc}) of DAP-M4/TPU film within 600s. (c) the simulated piezopotential difference between two electrodes of the DAP-M4/TPU film indicated by color gradient.